

Supporting information

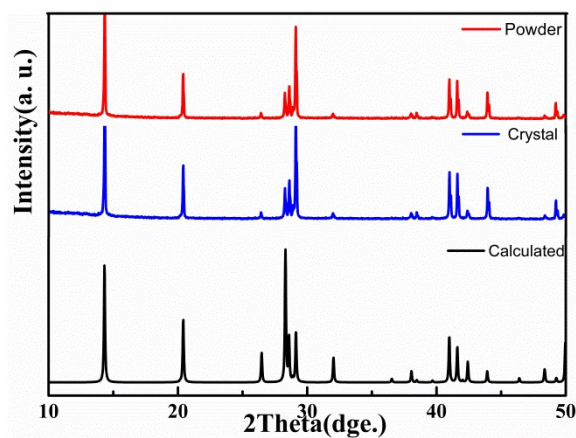


Fig. S1 Experimental and calculated powder X-ray diffraction patterns for polycrystalline and crystal LiVMo_6

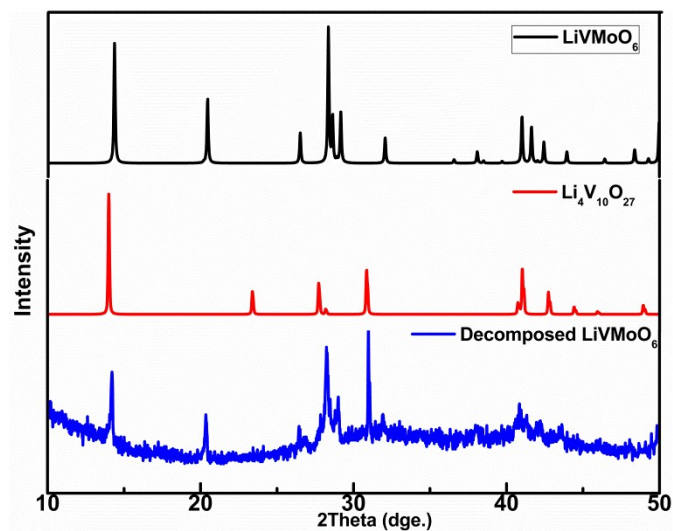


Fig. S2 Powder X-ray diffraction patterns for decomposed crystal LiVMo_6 .

Table S1 Crystal data and structure refinement for monoclinic LiVMoO₆

Empirical formula	LiVMoO ₆
Formula weight/g·mol ⁻¹	249.82
Temperature/K	296(2)
Wavelength/Å	0.71073
Crystal system, space group	Monoclinic, C2/m
Unit cell dimensions/Å	$a=9.3531(9)$, $b=3.6477(4)$, $c=6.647(7)$ $b=3.6477(4)$ $\alpha(\text{deg})=90^\circ$ $\beta(\text{deg})=111.6430^\circ$
Volume (Å ³)	210.79
Z	2
T(K)	296
Absorption coefficient, $\mu(\text{mm}^{-1})$	4.967
Theta range for data collection (°)	3.3 to 22.52
Limiting indices	$-12 \leq h \leq 12$, $-4 \leq k \leq 4$, $-8 \leq l \leq 8$
$R(\text{int})$	0.0139
Independent reflection	1251
Absorption correction	Semi-empirical from equivalent
Refinement method	Full-matrix least-squares on F ²
Goodness-of-fit on F ²	1.229
Final R indices [$I > 2\sigma(I)$] ^a	$R_1=0.0138$, $wR_2=0.0334$
R indices (all data)	$R_1=0.0123$, $wR_2=0.0332$
Extinction coefficient	0.0179(16)
largest diff. peak and hole ($e \cdot \text{Å}^{-3}$)	0.190 and -0.207

^a $R_1 = \sum ||F_o| - |F_c|| / \sum |F_o|$, $wR_2 = \{ \sum [w(F_o^2 - F_c^2)^2] / \sum [w(F_o^2)^2] \}^{1/2}$

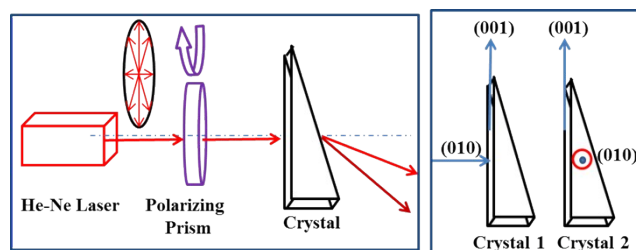


Fig. S3 Schematic of the experimental facilities to determined optical principle axes

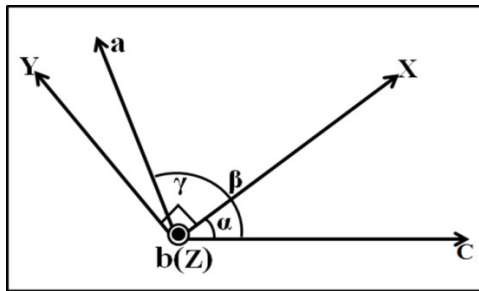


Fig. S4 Relative orientation of the optical axes (X , Y , and Z) with regard to the crystallographic axes (a , b , and c) for the monoclinic LiVMoO_6 single crystals, $\alpha=40^\circ$, $\beta=111^\circ$, $\gamma=90^\circ$

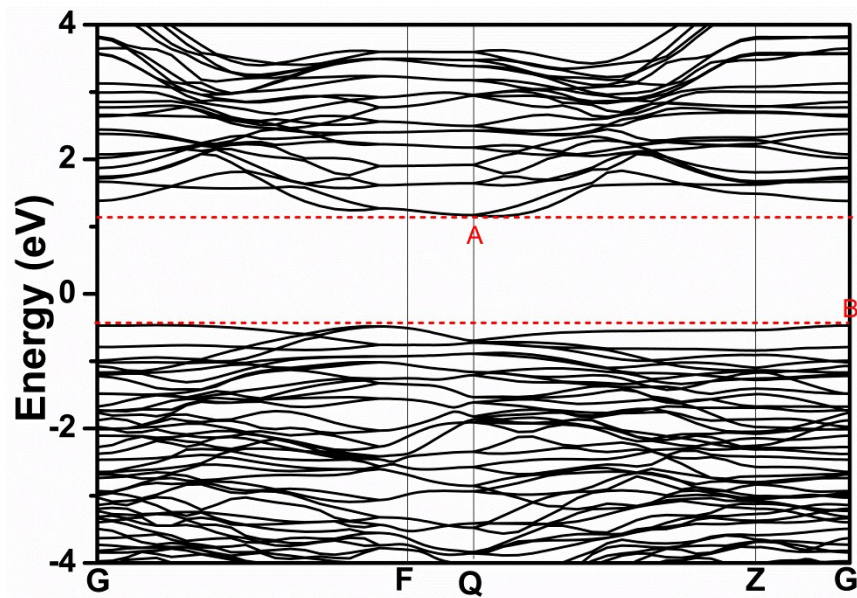


Fig. S5 The band structure of LiVMoO_6 near Fermi level. The lowest CB and the highest VB located at “A” and “B” respectively.